European Journal of Radiology 118 (2019) 271–276

Contents lists available at ScienceDirect

European Journal of Radiology

journal homepage: www.elsevier.com/locate/ejrad

Research article

7T TOF-MRA shows modulated orifices of lenticulostriate arteries associated with atherosclerotic plaques in patients with lacunar infarcts

Qingle Kong[a,b,c,1], Zihao Zhang[a,b,c,*,1], Qi Yang[d,e], Zhaoyang Fan[d], Bo Wang[a,b,c], Jing An[f], Yan Zhuo[a,b,c,*]

[a] State Key Laboratory of Brain and Cognitive Science, Institute of Biophysics, Chinese Academy of Sciences, 15 Datun Road, Beijing, 100101, China
[b] CAS Center for Excellence in Brain Science and Intelligence Technology, 15 Datun Road, Beijing, 100101, China
[c] University of Chinese Academy of Sciences, 19A Yuquan Road, Beijing, 100049, China
[d] Biomedical Imaging Research Institute, Cedars-Sinai Medical Center, 8700 Beverly Blvd, Los Angeles, CA, 90048-0750, United States
[e] Xuanwu Hospital, Capital Medical University, Beijing, 45 Changchun Street, Beijing, 100053, China
[f] Siemens Shenzhen Magnetic Resonance Ltd., Gaoxin C. Ave., 2nd, Shenzhen, 518057, China

ARTICLE INFO

Keywords:
Lenticulostriate vasculopathy
Magnetic resonance angiography
Magnetic resonance imaging
Lacunar infarcts
Intracranial atherosclerosis
7 Tesla

ABSTRACT

Purpose: To characterize the orifices of lenticulostriate arteries (LSAs) in vivo by using three-dimensional (3D) time-of-flight magnetic resonance angiography (TOF-MRA) and to investigate the spatial relationship between LSA orifices and atherosclerotic plaques in patients with lacunar infarcts (LI).

Method: Seventeen healthy volunteers and fifteen patients with LI underwent 3D TOF-MRA and 3D vessel wall imaging (VWI) at 7 T. The orifices of LSAs and the locations of atherosclerotic plaques on MCA walls were categorized based on the involvement of the superior, inferior, ventral or dorsal sides of MCA wall. The distribution quadrants of LSA orifices on MCA walls were compared among different groups.

Results: Most orifices were located on the superior side of MCA firstly (46 of 95, 48.4%), followed by the dorsal side (22 of 95, 23.2%). In patients with LI, the visible numbers of ventral and inferior orifices on the ipsilateral side were significantly lower than healthy controls ($p = 0.039$ for ventral side, $p = 0.002$ for inferior side). Similarly, plaques occurred more frequently at the ventral (7 of 20, 35.0%) and the inferior (7 of 20, 35.0%) sides of MCA walls.

Conclusions: TOF-MRA at 7 T is capable of imaging orifices of LSA on MCA. In patients with LI, the decreased number of LSA orifices on the ventral and inferior sides corresponded with the distribution of MCA plaques. The results may indicate the vulnerability of LSA orifices in intracranial atherosclerosis, which was supposed to be the cause of LI in basal ganglia.

1. Introduction

Lacunar infarcts (LI) resulting from the small penetrating arteries occlusion comprise ~20% of all strokes, a proportion similar to those resulting from large artery atherosclerosis or cardioembolism [1]. Lenticulostriate arteries (LSAs) are a collection of small perforating arteries that arise from the circle of Willis (CoW), supplying the basal ganglia (BG) and its vicinity in the brain [2]. Its impairment is considered to be the cause of LI in basal ganglia area [3] and vascular dementia [4]. Previous studies demonstrated that occlusion of LSA caused by artery-to-artery embolism and small vessel disease should be treated separately, as they have different pathologies [5]. However, because of small caliber and relatively slow blood velocity, the in vivo imaging method of LSA remains challenging in clinical settings. Digital subtraction angiography (DSA) is a feasible way of imaging LSA, but it cannot provide information of vessel wall lesions and infarcts on brain

Abbreviations: 3D, three-dimensional; 7T, 7 tesla; BG, basal ganglia; CoW, circle of willis; CT, computed tomographic; DSA, digital subtraction angiography; GRAPPA, generalized autocalibrating partially parallel acquisitions; LI, lacunar infarcts; LSA, lenticulostriate artery; MCA, middle cerebral artery; MIP, maximum intensity projections; MPRAGE, magnetization prepared rapid gradient echo; MRI, magnetic resonance imaging; SPACE, sampling perfection with application-optimized contrast using different flip angle evolutions; T1w, T1-weighted; TOF-MRA, time-of-flight magnetic resonance angiography; VWI, vessel wall imaging

* Corresponding authors at: State Key Laboratory of Brain and Cognitive Science, Beijing MR Center for Brain Research, Institute of Biophysics, Chinese Academy of Sciences, Bldg. 11, 15 Datun Road, Chaoyang District, Beijing, 100101, China.
E-mail addresses: zhzhang@ibp.ac.cn (Z. Zhang), yzhuo@ibp.ac.cn (Y. Zhuo).
[1] These authors contributed equally to this article.

https://doi.org/10.1016/j.ejrad.2019.07.032
Received 22 March 2019; Received in revised form 7 June 2019; Accepted 25 July 2019

parenchyma. As a result, LSA has not been extensively studied in LI, especially about its associations with atherosclerotic plaques on MCA.

Over the past few decades, the development of MRI greatly facilitated the study of stroke. The most prominent MRI techniques for imaging intracranial arterial pathologies are time-of-flight MR angiography (TOF-MRA) and vessel wall imaging (VWI). TOF-MRA has been widely used in imaging intracranial large arteries, and plays an important role in clinical diagnosis of cerebral vascular diseases [6,7]. At ultra-high field (7 T), TOF-MRA was proved to be an efficient method of imaging LSA, without the need of exogenous contrast agent [8]. On the other hand, 3D high-resolution VWI has been developed to characterize intracranial vessel walls, enabling reliable evaluation of atherosclerotic plaques in the CoW [9]. Several studies have demonstrated morphological changes of LSA in vascular diseases using TOF-MRA at 7 T [10,11], while others have studied the distribution of atherosclerotic plaques on MCA using VWI [12,13]. According to the evolution of intracranial atherosclerosis, the orifices of LSAs is vulnerable to nearby atherosclerotic plaques on its parent MCA [14]. However, no study has ever incorporated TOF-MRA and VWI at 7 T together to investigate the associations between the impairment of LSA and the plaques on MCA.

In this work, the feasibility of using TOF-MRA at 7 T to display the orifices of LSA originating from MCA is demonstrated. The orientational distributions of LSA orifices in LI patients and healthy volunteers are analyzed and compared. The relationships between the atherosclerotic plaques, the orifices of LSA in the LI are discussed.

2. Materials and methods

2.1. Patients

From January 2017 to December 2017, eighteen patients from Xuanwu Hospital were prospectively collected in the study. They were clinically diagnosed as lacunar infarcts by radiologists and neurologists. The patients were included for having (a) transient ischemic attack or stroke (b) lacunar infarction in BG area and (c) stenosis in MCA based on the findings of preceding computed tomographic (CT) or MRI examinations. Among them 3 patients with motion artifact in final images were excluded. The remaining 15 LI patients (11 males; aged 15–74 years; mean age 47 ± 16.3 years) were finally included in the analysis. Seventeen healthy volunteers were also recruited in the study (8 males; aged 33–63 years; mean age 42 ± 7.7 years). All the participants underwent 7 T MR scanning in a research institute. Informed consent approved by the local institutional review board was obtained from all participants.

2.2. Magnetic resonance imaging

MRI was performed on a whole-body human 7 T MR research system (Siemens Healthcare, Erlangen, Germany) equipped with a 32-channel head coil (Nova Medical, MA, USA). The imaging sequences and the main parameters were listed in Table 1. All patients underwent the whole imaging protocol. On healthy volunteers, only T1-weighted (T1w) magnetization prepared rapid gradient echo (MPRAGE) and TOF-MRA were collected.

Single-slab 3D TOF-MRA with 47 mm axial coverage was performed to image LSA and MCA. Before imaging the target vessels in high resolution, a low-resolution TOF-MRA with isotropic 0.80 mm voxel size and whole-brain coverage was applied as a localizer. The single-slab TOF-MRA with high resolution of $0.23 \times 0.23 \times 0.36\,mm^3$ was performed covering the MCA and the area of BG. The following protocol was used: repetition time (TR) = 15 ms, flip angle (FA) = 20°, echo time (TE) = 4.3 ms, 128 slices, field of view (FOV) = $180*135*47\,mm^3$, time of acquisition (TA) = 7 min 34 s. The generalized autocalibrating partially parallel acquisitions (GRAPPA) was employed with acceleration factor = 2.

An optimized prototype SPACE (sampling perfection with application-optimized contrasts using different flip-angle evolution) sequence was used for VWI. The following parameters were used: TR = 1200 ms, TE = 16 ms, voxel size = $0.40*0.40*0.40\,mm^3$, FOV = $181*181*141\,mm^3$, echo train length = 50, GRAPPA factor = 3, and TA = 10 min 29 s.

2.3. Data analysis

2.3.1. Image review

Preliminary review of the angiography was performed on a digital workstation by an independent neuroradiologist (Q.Y., 6 years of radiological experience) blind to patient data. Maximum intensity projection (MIP) of the 3D TOF-MRA was reconstructed in the axial direction, using the software provided with the MRI scanner. The scan would be repeated if motion artifacts were found in the images of TOF-MRA or VWI.

2.3.2. Analysis of LSA orifices

The pre-processing of data was performed using SPM12 (Wellcome Trust Centre for Neuroimaging, London, UK, http://www.fil.ion.ucl.ac.uk/spm) in Matlab (The Mathworks Inc, MA). The images of TOF-MRA and VWI were reoriented to achieve an AC-PC alignment based on individual T1w structural images. The 3D MIP of TOF-MRA was inspected, and the section views of the M1 segment were extracted where an LSA originated. The cross sections were built perpendicular to the center line of MCA in Simvascular [15], so that the orifices of LSAs could be readily identified in the plane. All cross-sections were classified based on the quadrants that the orifices located in (the superior, inferior, dorsal, or ventral side of MCA, see Fig. 1). In case the orifice was distributed in multiple quadrants, the quadrant with the maximal part of the orifice was chosen. The classification of orifices was accomplished by two independent readers (Z.H.Z., Q.Y.; 5 and 6 years of

Table 1
The imaging protocol at 7 T for patients with lacunar infarcts and healthy volunteers.

	T1w-MPRAGE*	TOF-MRA*	T1w-VWI	T2w-FLAIR
Purpose	Infarction	LSA	Plaques	Infarction
FOV (mm^3)	224 × 203 × 180	180 × 135 × 47	181 × 181 × 141	220 × 200 × 117
Resolution (mm^3)	0.70 × 0.70 × 0.70	0.23 × 0.23 × 0.36	0.40 × 0.40 × 0.40	0.57 × 0.43 × 3.00
TR (ms)	2200	15	1200	14000
TE (ms)	3.21	4.30	16	94
FA (°)	7	20	Variable**	120**
Slice PF	6/8	6/8	5/8	–
Phase PF	7/8	6/8	Off	Off
TA (min)	9:19	7:34	10:29	7:58

Abbreviations: T1w, T1-weighted; MPAGE, magnetization prepared rapid gradient echo; TOF, time of flight; MRA, magnetic resonance angiography; VWI, vessel wall imaging; T2w, T2-weighted; FLAIR, fluid-attenuated inversion recovery; PF, partial fourier.

* For healthy volunteers, only T1w-MPRAGE and TOF-MRA were acquired. The inversion time (TI) for T1w-MPRAGE was 1050 ms.

** For refocusing flip angles.

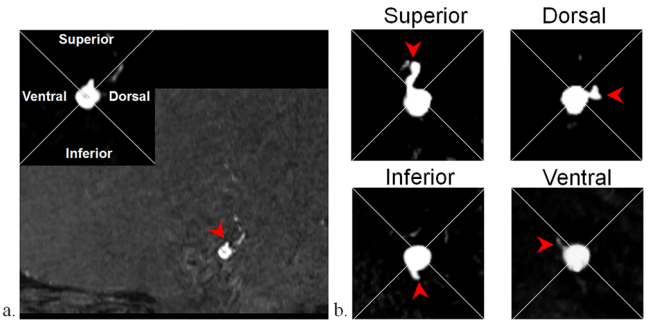

Fig. 1. The spatial distribution of LSA orifices on MCA. a), An alignment grid to demonstrate how each cross-section of M1 in TOF-MRA is divided into 4 quadrants. b) The classification of LSA orifices in the cross-sections of MCA. The arrows mark the orifices of LSA.

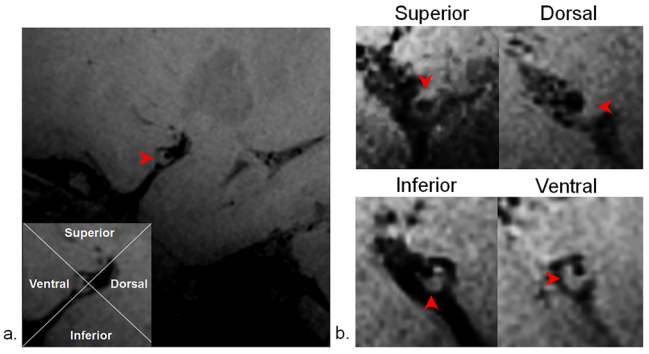

Fig. 2. The spatial distribution of atherosclerotic plaques on MCA walls. a) An alignment grid to demonstrate how each cross-section of M1 in VWI is divided into 4 quadrants. b) Examples of plaques involving the superior, inferior, ventral, or dorsal wall, respectively. The arrows mark the presence of plaques.

Table 2
Demographic, Clinical, and Plaque Characteristic of Patients.

Patient characteristic*	Value
Male sex	11 (73%)
Diabetes mellitus	1 (7%)
Hypertension	4 (27%)
Hyperlipidemia	1 (7%)
Chronic Stroke	15 (100%)
Transient ischemic attack	3 (20%)
No. of plaques identified (per patient**)	
1	3 (20%)
2	1 (7%)
3	2 (13%)
4	2 (13%)

* For the entire group of 15 patients.
** For the 9 patients with a chronic stroke (20 plaques).

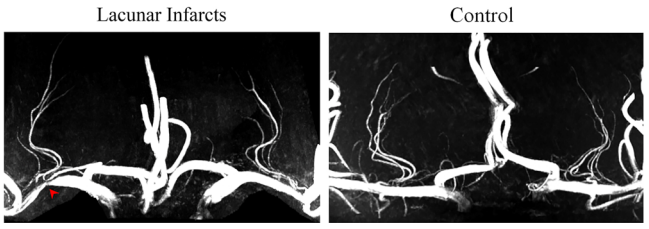

Fig. 3. The MIP images of 7 T TOF-MRA in an LI patient (stenosis in right MCA, red arrow) and a healthy volunteer.

experience in TOF-MRA, respectively). Cases with disagreement were reviewed together and resolved by consensus. The hemispheres of LI patients were divided into the ipsilateral group and the contralateral group based on the locations of their infarcts.

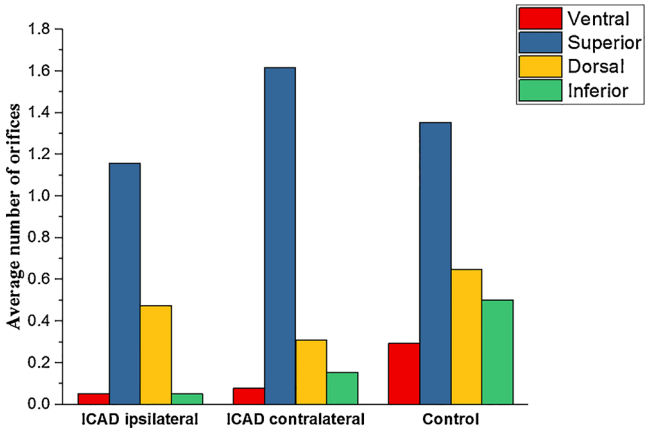

Fig. 4. The mean numbers of LSA orifices in the hemispheres of LI patients and healthy volunteers.

Table 3
The comparison of orifice numbers between patients and healthy control (*: $p < 0.050$, **: $p < 0.005$).

	Ventral	Superior	Dorsal	Inferior
LI ipsilateral vs. Control	0.039*	0.583	0.589	0.002**
LI contralateral vs. Control	0.120	0.302	0.221	0.133
LI ipsilateral vs. LI contralateral	0.784	0.078	0.437	0.342

2.3.3. Analysis of plaque distribution

Atherosclerotic plaque was defined as eccentric wall thickening with luminal stenosis (> 50%) identified on the reconstructed VWI images. The plaque was not counted if narrowing was only identified on the VWI images but not on the TOF-MRA images. Because only LSA originating from M1 segment was included in the analysis above, only plaques involving M1 segment of MCA were incorporated.

Cross-sections along the extracted vascular centerline were reconstructed in 3D VWI images. The locations of plaques on vessel walls were classified into four quadrants (the superior, inferior, dorsal, or ventral side of MCA, see Fig. 2). The number and the length of plaques in each quadrant was measured (see supplementary material). If a plaque was distributed in two quadrants simultaneously, each quadrant was counted separately. All the plaque-related analysis was executed in OsiriX [16]. The measurements were independently accomplished by two readers (Z.H.Z., Q.Y.; 3 and 6 years of experience in VWI, respectively). Final results were achieved by averaging their measurements.

2.3.4. Infarct characterization

T1w-MPRAGE and T2w-FLAIR were employed to identify infarcts in BG area, which was defined as low intensity in T1w images and high intensity in T2w images. The number and maximal diameter were recorded for the infarcts that were smaller than 1.5 cm in diameter and exclusively subcortical in location, which were defined as lacunae [17–19]. These infarcts are thought to be resulted from occlusion of small penetrating (e.g. LSA) branches of large cerebral arteries [18].

2.3.5. Statistical tests

The comparison of the orifice distribution among different walls was performed by a Kruskal-Wallis test followed by Bonferroni correction for multiple comparisons. In each quadrant, the number of orifices were compared among the ipsilateral side, contralateral sides of the LI patients and those of the control group. The Mann-Whitney U test was run between the test groups. The test groups include LI ipsilateral vs. control, LI contralateral vs. control, and LI ipsilateral vs. LI contralateral. A

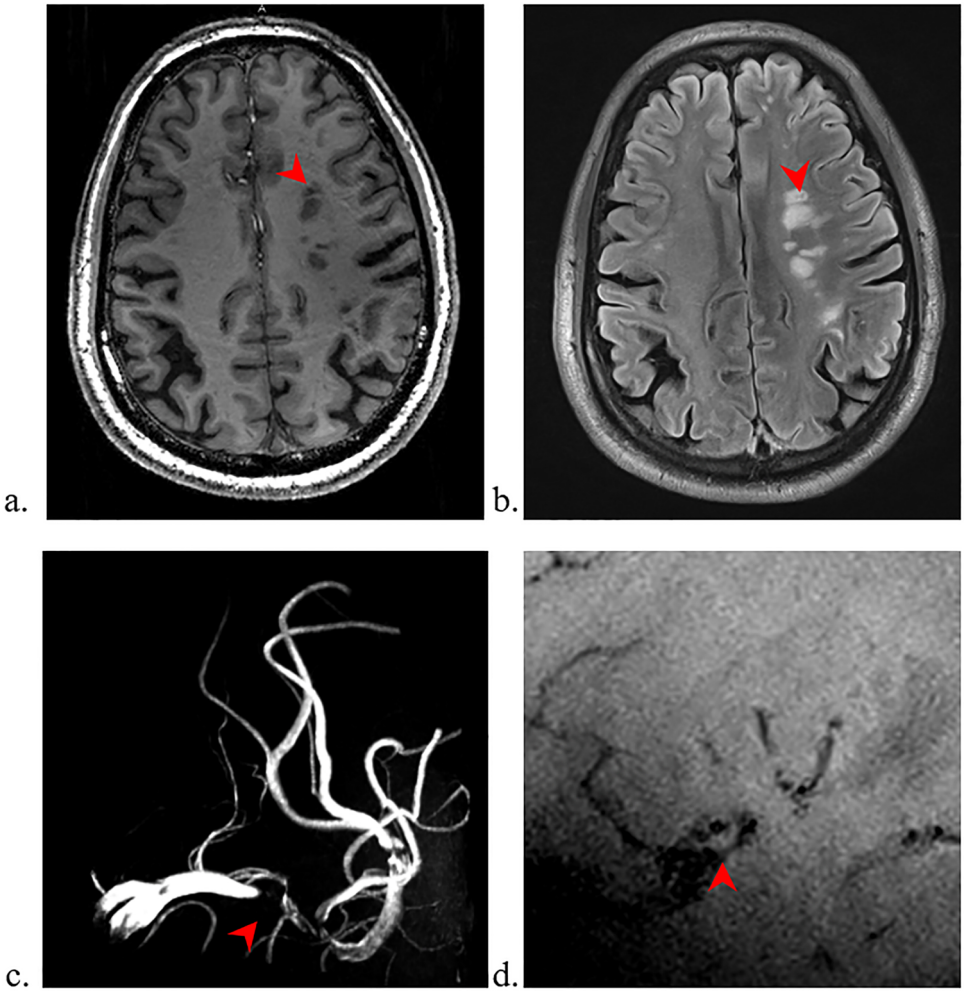

Fig. 5. Acute infarction downstream from a plaque-affected LSA orifice on the left MCA wall in a 74-year-old man. a) T1w MR image shows a hypointense signal intensity (arrow) in left parietal lobe. b) T2w FLAIR MR image shows corresponding hyperintense signal intensity (arrow). c) 3D TOF-MRA of the left hemisphere shows stenosis of the M1 segment (arrow). d) 3D VWI MR images show corresponding eccentric wall thickening in left M1 segment (arrow).

Table 4
The distribution of atherosclerotic plaques in M1 segments of the LI patients.

	Ventral	Superior	Dorsal	Inferior
Percentage of Occurrence	35.0 (7/20)	15.0 (3/20)	15.0 (3/20)	35.0 (7/20)
Mean Length	0.55 cm	0.40 cm	0.38 cm	0.69 cm

Note: Data in parentheses are numerator and denominator.

probability value less than 0.05 was considered statistically significant. Continuous variables were presented as means ± standard deviations.

3. Results

The clinical characteristics of the study population are shown in Table 2. All the fifteen LI had chronic stroke, and three had transient ischemic attacks.

The representative MIP images of 7 T TOF-MRA in a patient and a volunteer are shown in Fig. 3. According to the classification criteria in Fig. 1, the distribution of LSA orifices in the four quadrants is shown in Fig. 4. Most orifices were located on the superior side firstly, followed by the dorsal side. The superior side had more orifices of LSA than the other sides ($p < 0.01$, Kruskal-Wallis test; in supplementary material), in both volunteers and patients. The p values of Mann-Whitney U test on the numbers of orifices are listed in Table 3. In LI patients, the numbers of ventral ($p = 0.039$) and inferior ($p = 0.002$) orifices on the ipsilateral side were significantly lower than the healthy control, while the numbers on the contralateral side showed no significant differences from the control group. Acute infarction downstream from a plaque-affected LSA orifice on the MCA wall of left hemisphere in a 74-year-old man is shown in Fig. 5.

In order to explore the reasons for the different patterns of LSA orifices between the LI patients and healthy volunteers, we analyzed the distribution of plaques on the wall of M1 segment. A total of 20 plaques were identified in 9 patients. In all the fifteen patients, plaques causing > 50% stenosis in M1 segment were identified in 11 hemispheres. According to the classification criteria described above, plaques were more frequently located at the ventral (35.0%, 7 of 20) and the inferior (35.0%, 7 of 20) sides of vessel wall, while only 15.0% (3 of 20) were found at the superior and the dorsal sides. The mean lengths of plaque in the ventral and the inferior wall were also longer than those of the superior and dorsal wall, which is demonstrated in Table 4.

4. Discussion

In our study, we demonstrate for the first time that the orientation distribution of LSA orifices on MCA trunks can be visualized and analyzed noninvasively with high-resolution TOF-MRA at 7 T. Previous micro-anatomical studies suggested that most LSAs, which may be considered as flow dividers, arise dorsally from the upper part of MCA

wall [20]. Our *in vivo* study reports a consistent result that most orifices were located on the superior and the dorsal sides both in patients and in volunteers. The results showed that TOF-MRA at 7 T was a feasible tool for investigating intracranial perforating arteries, especially LSAs. In some cases, pulsation artifacts can be observed in the phase-encoding direction (see Supplementary Fig. 2), which was most obvious at axial slices and may be misinterpreted as a perforating artery. However, as our inspection of LSA orifices was performed on the continuous sagittal cross sections of MCA, pulsation artifacts can be easily distinguished from real lenticulostriate arteries and thus had no effect on our final results. Like other MRI methodologies, TOF-MRA was sensitive to motion artifacts that blurred the tiny branches of LSA. Shortening the acquisition time with advanced acceleration methods have great potential on increasing the probability of getting successful scanning.

For LI patients, the orifices of LSA are found affected mainly on the ipsilateral side, especially on the ventral and inferior parts of MCA wall. Due to the influenced pattern of orifices, the blood flow of LSA is mostly supplied through the superior branches in LI patients. Among the patients included in our study, plaques are observed predominantly in the ventral and inferior wall. Similar distribution pattern of plaques on MCA was previously reported in a study of atherosclerotic MCA stenosis [12]. The results provided by TOF-MRA and VWI demonstrate that orifices of LSA is vulnerable to the plaques on MCA. The change of LSA orifices in the ipsilateral hemisphere indicate the stenosis or occlusion of LSA may be the cause of the lacunar infarcts, which was first reported in-vivo using a noninvasive imaging method.

The findings may be meaningful in the etiological study of LI. The forceful displacement of neighboring atheromatous material into the ostia of arterial branches was a major concern of intracranial angioplasty [21]. Before this study, there was no report studying the orifices of LSA. In a previous study, as the LSA could not be evaluated with TOF-MRA at 3 T, the displacement of neighboring atheromatous material into branch vessel ostia was speculated to be uncommon [12]. In this study, all MRI scans were performed on a 7 T MR system. In MRI, the signal to noise ratio (SNR) increased proportionally with the magnetic field strength, and is the most important factor deciding the resolution. Another advantage of ultra-high field MRA is that T_1 relaxation becomes longer under higher field, which improves the flow related enhancement in TOF-MRA and produces the longer visible length in small arteries like LSA [8]. Because of the capability of imaging and analyzing the angiography of LSA and the vessel wall of MCA, the consistency was revealed successfully between the injured orifices of LSA and the prone locations of atherosclerotic plaques. The results, to a certain extent, demonstrate that the ostia of LSA were vulnerable to the displacement of atheromatous material. The spatial information of the LSA orifices and the atherosclerotic plaques should therefore be seriously considered in the interventional therapy and the neurological management of patients with cerebral vascular diseases, to decrease the risk of the secondary collusions in perforation arteries.

In conclusion, we have shown that the orifices of LSA may be visualized and analyzed using TOF-MRA at 7 T. The spatial relationship between the orifices of LSA and the atherosclerotic plaques indicates that the LSA was vulnerable to the atherosclerotic plaques on MCA in LI patients. The high-resolution TOF-MRA and VWI at 7 T may lead to a better understanding of the progression of cerebral arterial diseases, especially how the plaque in the Circle of Willis cause ischemic stroke in basal ganglia areas.

Funding

This work was supported by Beijing Municipal Natural Science Foundation (7184226), Young Elite Scientists Sponsorship Program by CAST (2017QNRC001), the Ministry of Science and Technology of China grant (2015CB351701), the National Nature Science Foundation of China grant (31730039), and the Chinese Academy of Sciences grant (XDBS32000000).

Dr. Jing An is an employee of Siemens Healthcare. The other authors have no conflicts of interest to be disclosed related to this article. The Institute of Biophysics (Chinese Academy of Sciences) holds a research agreement with Siemens Healthcare, who provided the SPACE work-in-progress MRI sequence.

Declaration of Competing Interest

Dr. Jing An is an employee of Siemens Healthcare. The other authors have no conflicts of interest to be disclosed related to this article. The Institute of Biophysics (Chinese Academy of Sciences) holds a research agreement with Siemens Healthcare, who provided the SPACE work-in-progress MRI sequence.

Appendix A. Supplementary data

Supplementary material related to this article can be found, in the online version, at doi:https://doi.org/10.1016/j.ejrad.2019.07.032.

References

[1] C. Sudlow, C. Warlow, Comparable studies of the incidence of stroke and its pathological types results from an international collaboration, Stroke 28 (1997) 491–499, https://doi.org/10.1161/01.str.28.3.491.
[2] G. Gold, E. Kovari, P.R. Hof, C. Bouras, P. Giannakopoulos, Sorting out the clinical consequences of ischemic lesions in brain aging: a clinicopathological approach, J. Neurol. Sci. 257 (2007) 17–22, https://doi.org/10.1016/j.jns.2007.01.020.
[3] A.I. Qureshi, S. Tuhrim, J.P. Broderick, H.H. Batjer, H. Hondo, D.F. Hanley, Spontaneous intracerebral hemorrhage, N. Engl. J. Med. 344 (2001) 1450–1460, https://doi.org/10.1056/NEJM200105103441907.
[4] G.C. Román, T. Erkinjuntti, A. Wallin, L. Pantoni, H.C. Chui, Subcortical ischaemic vascular dementia, Lancet Neurol. 1 (2002) 426–436, https://doi.org/10.1016/S1474-4422(02)00190-4.
[5] J.M. Wardlaw, E.E. Smith, G.J. Biessels, et al., Neuroimaging standards for research into small vessel disease and its contribution to ageing and neurodegeneration, Lancet Neurol. 12 (2013) 822–838, https://doi.org/10.1016/S1474-4422(13)70124-8.
[6] J.P. Villablanca, K. Nael, R. Habibi, A. Nael, G. Laub, J.P. Finn, 3T contrast- enhanced magnetic resonance angiography for evaluation of the intracranial arteries: comparison with time-of-flight magnetic resonance angiography and multislice computed tomography angiography, Invest. Radiol. 41 (2006) 799–805, https://doi.org/10.1097/01.rli.0000242835.00032.f5.
[7] J.C. Ferre, B. Carsin-Nicol, X. Morandi, et al., Time-of-flight MR angiography at 3T versus digital subtraction angiography in the imaging follow-up of 51 intracranial aneurysms treated with coils, Eur. J. Radiol. 72 (2008) 365–369, https://doi.org/10.1016/j.ejrad.2008.08.005.
[8] Z.H. Cho, C.K. Kang, J.Y. Han, et al., Observation of the lenticulostriate arteries in the human brain in vivo using 7.0T MR angiography, Stroke 39 (2008) 1604–1606, https://doi.org/10.1161/STROKEAHA.107.508002.
[9] Y. Qiao, D.A. Steinman, Q. Qin, et al., Intracranial arterial wall imaging using three-dimensional high isotropic resolution black blood MRI at 3.0 Tesla, J. Magn. Reson. Imaging 34 (2011) 22–30, https://doi.org/10.1002/jmri.22592.
[10] S.W. Seo, C. Kang, S.H. Kim, et al., Measurements of lenticulostriate arteries using 7T MRI: new imaging markers for subcortical vascular dementia, J. Neurol. Sci. 322 (2012) 200–205, https://doi.org/10.1016/j.jns.2012.05.032.
[11] C.K. Kang, C.A. Park, C.W. Park, Y.B. Lee, Z.H. Cho, Y.B. Kim, Lenticulostriate arteries in chronic stroke patients visualised by 7 T magnetic resonance angiography, Int. J. Stroke 5 (2010) 374–380, https://doi.org/10.1111/j.1747-4949.2010.00464.x.
[12] W. Xu, M. Li, S. Gao, et al., Plaque distribution of stenotic middle cerebral artery and its clinical relevance, Stroke 42 (2011) 2957–2959, https://doi.org/10.1161/STROKEAHA.111.618132.
[13] B. Huang, W. Yang, X. Liu, H. Liu, P. Li, H. Lu, Basilar artery atherosclerotic plaques distribution in symptomatic patients: a 3.0 T high-resolution MRI study, Eur. J. Radiol. 82 (2013) 199–203, https://doi.org/10.1016/j.ejrad.2012.10.031.
[14] Y. Yoon, D.H. Lee, D.W. Kang, S.U. Kwon, J.S. Kim, Single subcortical infarction and atherosclerotic plaques in the middle cerebral artery, Stroke 44 (2013) 2462–2467, https://doi.org/10.1161/STROKEAHA.113.001467.
[15] A. Updegrove, N. Wilson, J. Merkow, H. Lan, A.L. Marsden, S.C. Shadden, SimVascular: an open source pipeline for cardiovascular simulation, Ann. Biomed. Eng. 45 (2017) 525–541, https://doi.org/10.1007/s10439-016-1762-8.
[16] A. Rosset, L. Spadola, O. Ratib, OsiriX: an open-source software for navigating in multidimensional DICOM images, J. Digit. Imaging 17 (2004) 205–216, https://doi.org/10.1007/s10278-004-1014-6.
[17] W.T. Longstreth, C. Bernick, T.A. Manolio, N. Bryan, C.A. Jungreis, T.R. Price, Lacunar infarcts defined by magnetic resonance imaging of 3660 elderly people: the Cardiovascular Health Study, Arch. Neurol. 55 (1998) 1217–1225, https://doi.org/10.1001/archneur.55.9.1217.
[18] C.M. Fisher, Lacunar strokes and infarcts a review, Neurology 32 (1982) 871–876,

https://doi.org/10.1212/wnl.32.8.871.
[19] A.G. Osborn, K.L. Salzman, M.D. Jhaveri, A.J. Barkovich, Diagnostic Imaging: Brain E-Book, Elsevier Health Sciences, 2015.
[20] F. Umansky, F. Gomes, M. Dujovny, et al., The perforating branches of the middle cerebral artery: a microanatomical study, J. Neurosurg. 622 (1985) 261–268, https://doi.org/10.3171/jns.1985.62.2.0261.
[21] E.I. Levy, S. Chaturvedi, Perforator stroke following intracranial stenting: a sacrifice for the greater good? Neurology 66 (2006) 1803–1804, https://doi.org/10.1212/01.wnl.0000227198.02597.15.